SPECIAL REPORT 95-7

CRREL

Detection of Crevasses Near McMurdo Station, Antarctica With Airborne Short-Pulse Radar

Allan J. Delaney and Steven A. Arcone

March 1995

Abstract
Airborne short-pulse radar is evaluated experimentally as a rapid reconnaissance tool for locating snow-bridged crevasses. An immediate need for a crevasse detector is present within the U.S. Antarctic Program, which is planning a major surface traverse from McMurdo to deliver construction materials to South Pole Station. This feasibility study of a crevasse detection system was performed near McMurdo Station, Antarctica, in January 1994. The radar utilized pulses centered near 200 and 500 MHz and was operated from a low flying helicopter with altitude and speed as variables. A global positioning system (GPS) was used for survey control. Results are presented over glacial ice on Ross Island and at various locations on the Ross Ice Shelf near White and Black Islands and near the Aurora Glacier terminus. These studies include a control line along which crevasse width and snow-bridge thickness were measured, transects along which crevasses were apparent, and also where crevasses were expected, but were not apparent. Strong evidence of crevassing was recorded at flight speeds near 20 m s^{-1} (45 mph), at altitudes near 15 m, and at a data acquisition rate of 51 scans/second. Crevasses are detected by the reflections and diffractions from distorted layering in snow bridges, and by the strong diffractions from within the crevasses. The strongest diffractions apparently emanated from within the crevasse and not from the base of the snow bridge. Along the control line, a crevasse with no surface expression was detected by radar and verified by probing and digging. Transects devoid of crevasses show layering without the small scale distortion seen over snow bridges. Future plans are to use data acquisition rates of 160 scans/second, available with commercial equipment, to allow a survey speed of about 64 m s^{-1} (140 mph). We believe that quality data could then be acquired at altitudes up to about 30 m, making short pulse radar a useful crevasse mapping tool from fixed wing aircraft.

For conversion of SI metric units to U.S./British customary units of measurement consult ASTM Standard E380-89a, *Standard Practice for Use of the International System of Units,* published by the American Society for Testing and Materials, 1916 Race St., Philadelphia, Pa. 19103.

Special Report 95-7

U.S. Army Corps of Engineers
Cold Regions Research & Engineering Laboratory

Detection of Crevasses Near McMurdo Station, Antarctica With Airborne Short-Pulse Radar

Allan J. Delaney and Steven A. Arcone

March 1995

Accesion For	
NTIS CRA&I	☑
DTIC TAB	☐
Unannounced	☐
Justification	
By	
Distribution /	
Availability Codes	
Dist	Avail and / or Special
A-1	

Prepared for
NATIONAL SCIENCE FOUNDATION

PREFACE

This report was prepared by Allan J. Delaney, Physical Science Technician, and Dr. Steven A. Arcone, Geophysicist, of the Snow and Ice Division, Research and Engineering Directorate, U.S. Army Cold Regions Research and Engineering Laboratory.

The National Science Foundation provided funding and logistical support for this study as part of the CRREL engineering investigations in Antarctica (Project T-310). Aircraft support was provided by the U. S. Navy Antarctic DEVRON Six. The authors thank Simon Stephenson and Frank Brier for their interest in the study, Steve Dunbar and the staff of the Berg Field Center for assistance both on the ground and in the air, Paul Sellmann and George Blaisdell of CRREL for technically reviewing the report, and Pamela Hill for coordinating all of the helicopter support.

Detection of Crevasses Near McMurdo Station, Antarctica with Airborne Short-Pulse Radar

ALLAN J. DELANEY AND STEVEN A. ARCONE

INTRODUCTION

The National Science Foundation is currently evaluating several methods of remote sensing and reconnaissance to aid in selecting an over-ice traverse route to South Pole Station. One obstacle to route planning is crevasses, which often have no visible surface expression to warn of their presence yet can be wide enough and deep enough to engulf a tractor. Since detection systems towed slowly along the snow surface give little advance warning of crevasse danger to the survey vehicle, airborne systems are needed for survey safety, reconnaissance, and efficient data collection. This report discusses the results of some observations using airborne short-pulse radar for detecting crevasses.

Early evidence that surface-based short-pulse radar easily detects near-surface crevasses from their diffractions was presented by Kovacs and Abele (1974). They pushed a 100-MHz transducer along the snow surface with a tracked vehicle at 1.4 m s^{-1} (3 mph) and recorded a diffraction from a suspected crevasse (Fig. 1). While this transducer configuration can be used for crevasse detection and warning at slow vehicle speeds, it is not suitable for reconnaissance surveys and cannot provide information to the surface vehicle as to which direction to steer to avoid a crevasse.

The objective of this study was to evaluate the use of short-pulse radar as a rapid reconnaissance tool for locating and mapping the extent of snow-bridged crevasses from aircraft. Helicopter-mounted radar transducers, along with a satellite global positioning system (GPS) antenna, were flown over several areas of known crevassing in the McMurdo Station area of Antarctica. Several crevasse fields were studied, one of which was directly explored by probing and digging.

The ability of short-pulse radar on low flying helicopters to obtain profiles of snow and ice thickness (Kovacs 1978, Arcone and Delaney 1987, Arcone 1991, Arcone et al. 1992, Vickers et al. 1973), sea ice thickness (Kovacs 1977) and frost penetration beneath frozen rivers (Delaney et al. 1990), and to locate winter water supplies in the Arctic (Arcone et al. 1989) suggested to us that airborne crevasse detection would be feasible. In particular the 500-MHz glacial data of Arcone et al. (1992) revealed many diffractions beneath a snow cover that suggested crevasse detection would be feasible at such short wavelengths. What was not apparent was how the data would be affected by the aircraft speed coupled with the limited scan rate, the low directivity of the radar transducer, and aircraft altitude.

TECHNIQUES AND EXPERIMENTAL PROCEDURE

The Antarctic provides an ideal environment in which to use short-pulse radar for subsurface exploration and reconnaissance. The low permittivity of cold snow and ice, the low variability of material electrical properties, and the absence of complex surface conditions allow good signal penetration. Although the contrasts in dielectric permittivity ε between air, dense snow, and ice are small (1, 2, and 3.2, respectively, at very high frequencies), the use of high-gain receivers overcomes the low amplitude of the reflected signals and makes it possible to detect air-filled voids in cold snow. In this study we utilized 200- and 500-MHz short-pulse radar transducers with transmitted pulse lengths of 5 and 2 ns respectively, and time ranges of 300 to 120 ns to record subsurface reflections. A 300-ns time range allows signal pen-

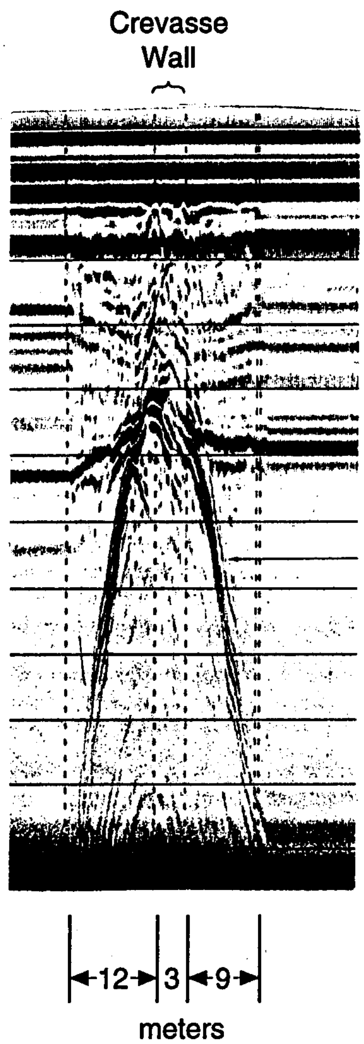

Figure 1. Diffraction pattern recorded by pushing a 100-MHz transducer along the snow surface in front of a tracked vehicle at a speed of 1.4 m s^{-1} (after Kovacs and Abele, 1974).

etration to a depth of over 20 m at a low altitude of a few meters, and the short pulse length of 2 ns at 500 MHz affords high vertical resolution.

Radar system

The short-pulse radar system consisted of a control unit (GSSI model 4800), data recorder (GSSI model DT-6000) and high frequency radar transducers (GSSI model 3107 at 200 MHz and model 3102 at 500 MHz). The radar control unit triggers pulses at a repetition frequency of 50 kHz and data were recorded in 8-bit, 512-word scans at a rate of 25.6 or 51.2 per second. The received radio frequency signals are sampled and converted to audio frequencies for display and recording on tape. The reconstructed signal is then displayed over a selected calibrated time range window. Variable time range gain may be applied to the audio scan to suppress the higher amplitude early returns, especially from the transducer direct coupling, and enhance the lower amplitude later returns that originate at layer interfaces and material transitions.

The antennas used are resistively loaded, bowtie dipoles. The 500-MHz transducer contains separate transmitter and receiver antennas backed by metallic shielding that greatly reduces side and back radiation. Consequently, aircraft reflections, or "clutter," are greatly reduced. The 200-MHz transducer contains one antenna and a transceiver (a monostatic configuration). Although it is shielded, extra oscillations occur when metallic struts are attached to the antenna housing.

In air the antenna beam width becomes fairly uniform with a 3- and 10-dB width of about 70° and 120° respectively. It is this wide beam width that allows diffractions from crevasses to be seen in the records. Since the amplitude of the signal reflected from air, snow, and ice horizons is very small, we used high-gain receivers. In some cases this increased gain also amplified sampling noise and spurious interference from aircraft electronics. Transient interference from the aircraft radar altimeter was seen on one flight when the device had to be used because of poor visibility. Reflections from the airframe, and low frequency system noise were removed with well-known digital filtering techniques.

Data processing and interpretation

The 200-MHz data were first passed through a horizontal (scan-to-scan) "background removal" filter that eliminated aircraft reflections that occur at a constant time delay. This process marginally affected the ice data because changes in altitude prevent the data from being sensitive to the filter. All data were passed through a high-pass filter to remove d.c. offsets within individual scans and a low-pass filter to alleviate high frequency noise. Transformation of echo time delay into depth is generally based on the simple echo delay formula for flat interfaces or point reflectors:

$$d = ct/2\sqrt{\varepsilon} \tag{1}$$

where

d = the depth of a reflector in centimeters,
t = the echo time delay in ns,

c = the speed of electromagnetic waves in a vacuum (30 cm/ns) and

ε = the dielectric permittivity of the propagation medium.

The factor of two accounts for the round-trip propagation path. A value of $\varepsilon = 2$ was used to translate echo time delay into snow and firn depth. This value is based on the Ross Ice Shelf near-surface density profiles of Kovacs et al. (1982, 1993) and the density/dielectric permittivity calibration of Cumming (1952).

A reflection profile reveals three types of images of geophysical events. The most common are flat, gently sloping or undulating horizons that represent coherent reflections from a continuous interface such as the snow surface or a subsurface layer. A second type of event consists of concave down, hyperbolic images that represent diffractions from local discontinuities in dielectric properties. These events are sought here because they are generated by the sharp transitions from air to firn or ice that occur in crevasses. The third type of event is incoherent backscatter or radar system noise that is speckled throughout the record. Unwanted reflections such as those from a helicopter can often be eliminated by filtering when the reflections are at a constant time delay. Data are displayed, as echo time-of-return vs. profile distance, using a line intensity format that uses a nonlinear scheme of gray scale intensity that emphasizes weaker events. Profiles were printed on a Hewlett-Packard Paintjet printer. The quality of the printout was generally very good, but inferior to the display on the computer monitor.

Aircraft, flight speed and altitude

The radar system was controlled from a Bell UH-1N helicopter operated by the US Navy Antarctic DEVRON Six for the National Science Foundation. The transducer, GPS antenna, and their supports were attached to fuselage port-side hardpoints. The control units and power supply were operated from the rear passenger area. The survey altitude was 3–15 m and air speed was 5 to 20 m s^{-1}. Speed was estimated from aircraft instrumentation.

Flight speed was limited by the rate of data acquisition. With the control unit used for these studies set to the fastest rate possible (about 50 scans/sec), a helicopter speed of about 20 m s^{-1} (45 mph) would provide 2.5 scans for each meter of travel. This translates to about 25 scans over a 10-m-wide crevasse, which is about the widest we expected. At least 25 scans are needed to recognize a diffraction, but more were obtained even on small features because diffractions extend beyond the crevasse area.

Altitude above terrain and the survey line separation are directly related. Altitude is determined by the radar time range, and survey line spacing by the antenna beam width (approximately 70 conical degrees in air). For an altitude of 10 m then, survey lines should be spaced no more than 14 m apart for 100% coverage of the surface. In practice, we found the crevasse features to be so large, > 5 m across, that speed could be further increased and that closely spaced lines were not required. Therefore, our survey lines were separated about 20 m and we successfully acquired data at speeds up to 20 m s^{-1}, although most of the data were collected at speeds of 5 to 10 m s^{-1}.

Position control

Survey position control was provided by a Garmin 100 global positioning system (GPS) receiver using an external antenna mounted atop the radar transducer. The GPS acquires an initial position within several minutes and then updates position once every second. Position waypoints were manually recorded at the ends of all survey lines and incrementally on long survey lines coincidentally with event markers entered onto the radar data file. All of the GPS data recorded are listed in Appendix A.

RESULTS

The study sites were selected from air photos and by visual inspection from aircraft (Fig. 2). The site near Castle Rock contained an ice fall where surface ridges indicative of snow-bridged crevasses were apparent. Crevasses are known to exist at the site east of White Island but were not apparent. Very large crevasses were seen along a line south of White Island but not along a section of the tractor trail east of Black Island. The longer lines extending north from the terminus of the Aurora Glacier and east from White Island were flown in anticipation of transitions in ice conditions. All of the sites on the Ross Ice Shelf are further distinguished by varying snow accumulation rates.

Ice fall site

This heavily crevassed site is located on glacial ice approximately 1 km east of the Castle Rock trail. It was selected because crevasses are easily identified by the pronounced snow-bridge mar-

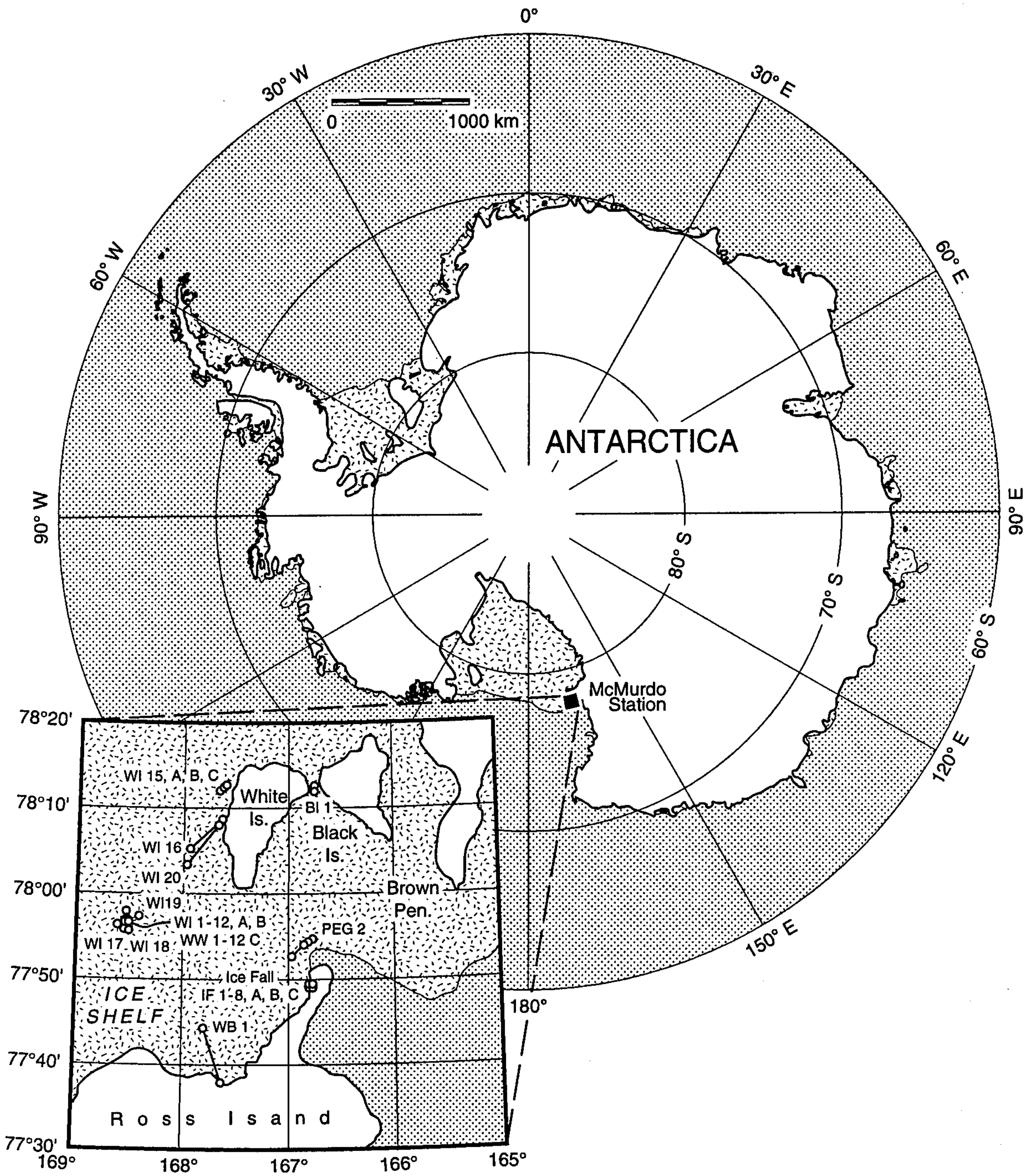

Figure 2. Location map showing Ross, Black and White Islands near McMurdo Station. The sites are located on glacial ice on Ross Island and at various locations on the Ross Ice Shelf.

gins. Eight lines were established by placing end flags from a hovering helicopter and an additional control line was established on the surface. All of the survey lines crossed the several obvious snow-bridged crevasses. Preliminary radar profiles were first recorded at an altitude of about 5 m at both 200 and 500 MHz. Some of the preliminary data recorded were at 200 MHz (above lines IF-3, 4, 5, and 6, Fig. 2) and are shown in Figure 3. The records are characterized by reflections from layers in the snow and ice and diffractions that seem to originate in the vicinity of crevasses seen during the flight. Profiles IF-3 and IF-5 contain event marks recorded when the transducer passed the obvious crevasse edges.

Based on these preliminary results a control line

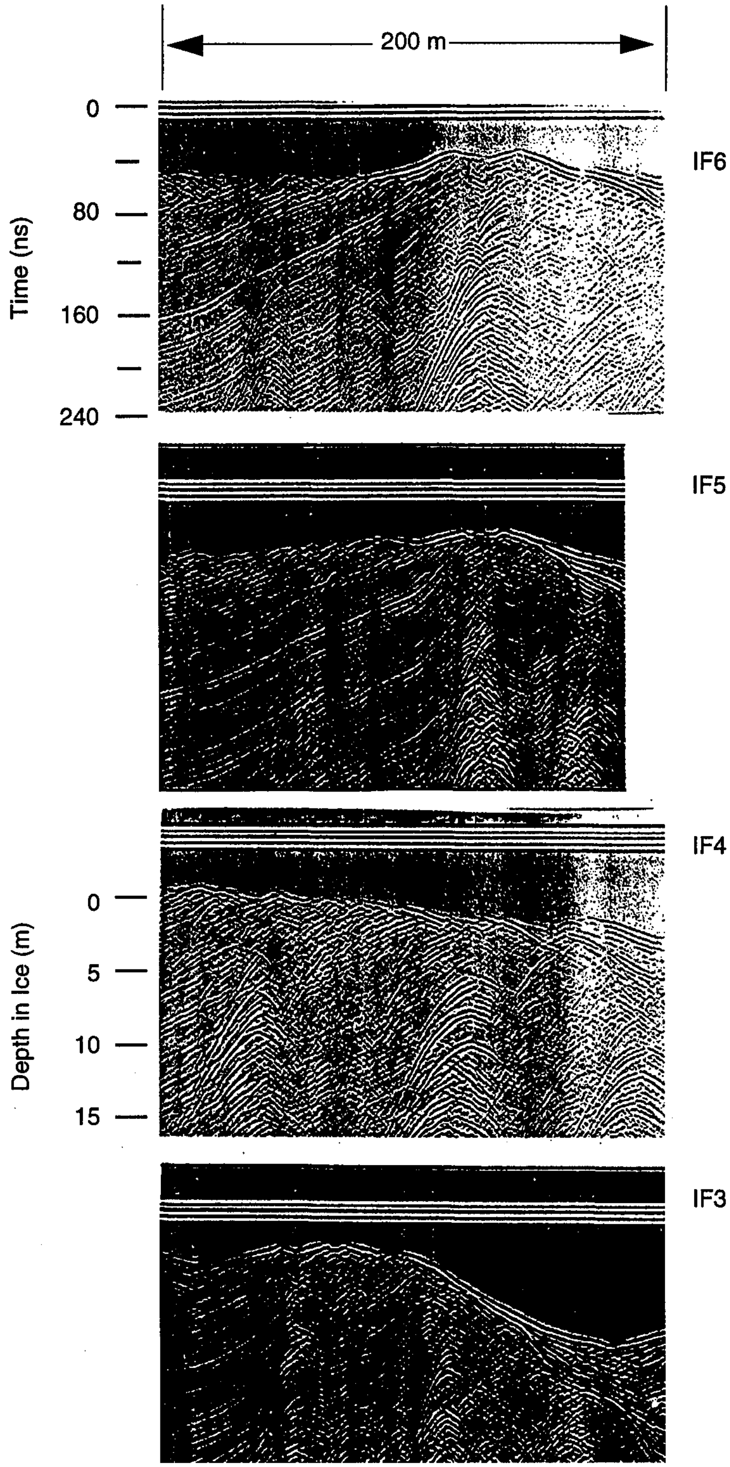

Figure 3. Preliminary 200-MHz profiles recorded above Ice Fall lines 3 through 6. The hyperbolic images are diffractions from crevasses. The wavy surface is due to changes in aircraft altitude. Aircraft speed was about 5 m s^{-1} and altitude varied from about 5 to 21 m.

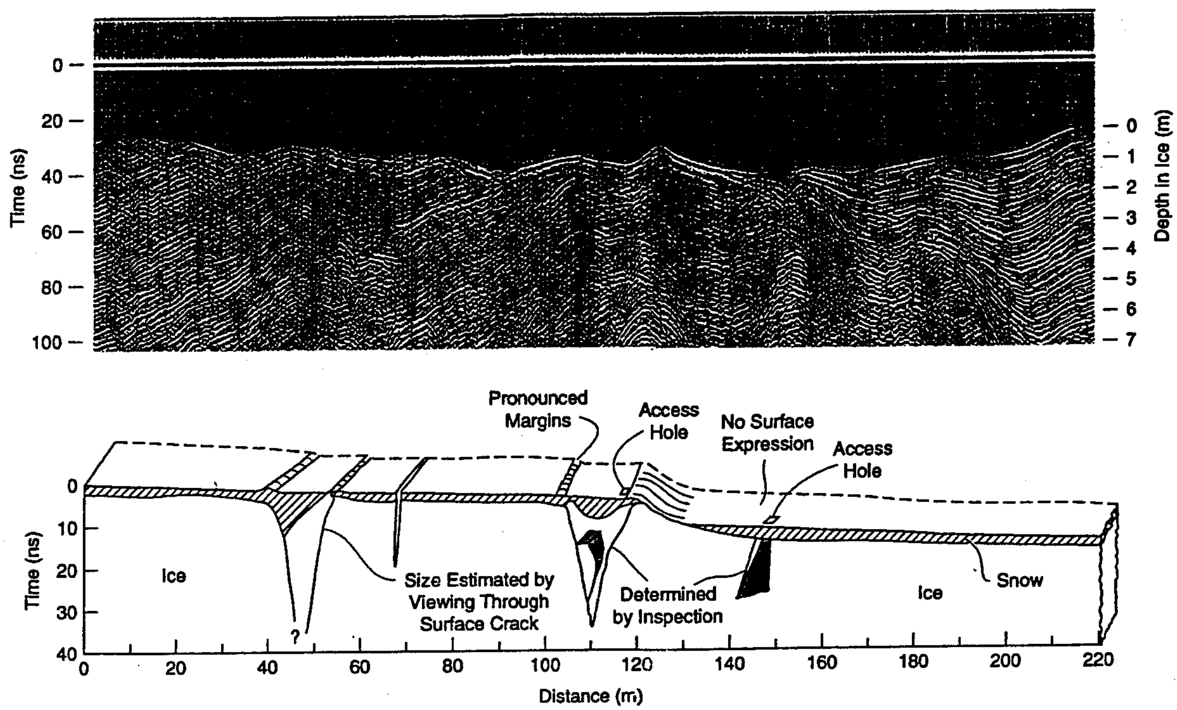

Figure 4. The 500-MHz profile recorded directly above the control line at a 120-ns time range. The cross section is interpreted from measurements made on the ground.

was established in the vicinity of lines 4 and 5 with the assistance of personnel from the Berg Field Center in McMurdo. This 215-m line crossed perpendicular to the several obvious snow-bridged crevasses and was flagged at 10-m intervals. Snow-bridge thickness was measured from augured holes, and crevasse dimensions were estimated after rappelling into the voids. Two large snow-bridged crevasses were found between 42–55 m and 105–120 m and an additional 1-m-wide crack occurred at 69 m (Fig. 4). The large crevasses contained asymmetric accumulations of snow and ice, which may explain the appearance of strong diffractions at only one edge of the feature centered at 110 m on the radar record.

The control line was then flown using the 500-MHz transducer and a time range of 120 ns to provide more detail of the near-surface features (Fig. 4). The survey altitude was about 5 m and speed was approximately 5 m s^{-1}. This profile should be compared with the 300-ns, 200-MHz profiles along lines 4 and 5 (Fig. 3), which provided less complicated and more apparent responses to the large voids at 50, 110, and 150 m. The shorter time range of Figure 4 shows near-surface features that may be related to snow-bridge dimensions and snow-ice transitions. Near-surface reflections seem to correspond with snow-bridge dimensions above the voids at 110 and 150 m.

Both radar profiles showed strong diffractions that corresponded with no observable surface features at 150 and 175 m. We therefore returned to station 150, where there was no surface expression of a crevasse, and dug through a 2.2-m-thick snowbridge to reveal a void 5 m wide at the top, 10 m wide at depth, and that extended 15 m below the surface. A similar feature may exist at 175-m distance at a time delay of 40 ns. The depth to this interface should be between 3.4 and 4.0 m, depending upon the probable range of material permittivity.

White Island tractor site

This site, east of White Island on the Ross Ice Shelf, was selected because snow-bridged crevasses were known to exist, but are not easily seen. The objective was to record data along parallel profiles from which we could map subsurface features. Flags mark the general location where a LGP D8 tractor fell through a snow bridge into a crevasse in 1991 and remains an estimated 18 m below the surface. There is very little surface relief and, under poor light conditions, we (on the aircraft) found it difficult to detect any surface patterns

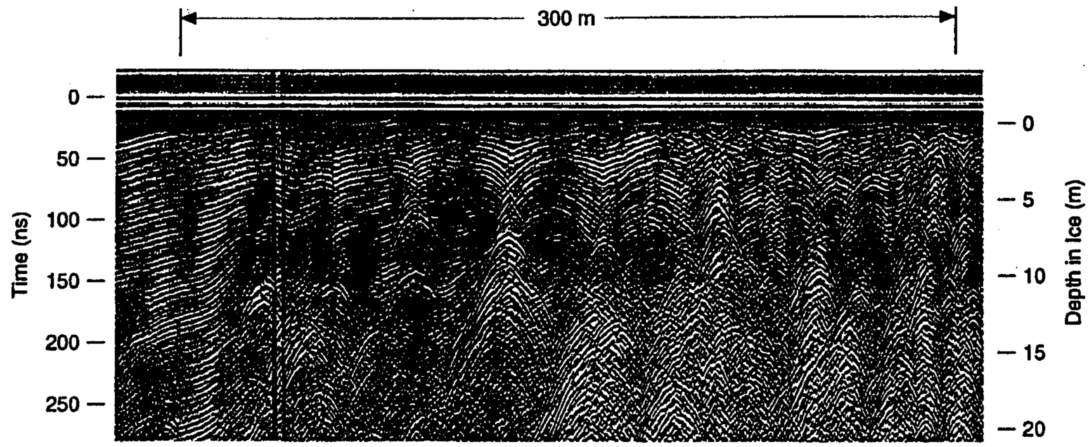

Figure 5. Data recorded above line 4 (WW-4C) at the White Island tractor site with the 200-MHz transducer.

indicating crevasses. When the aircraft climbed to about 300 m some widely spaced patterns in the snow surface became apparent. Ten parallel survey lines that crossed the marked tractor site were then established by placing end flags from the hovering helicopter. The lines were 300 m in length, and separated by 20 m (Fig. 2). GPS waypoints were also recorded at the end of each line.

The 10 parallel lines and the two additional end lines were flown at both 200 and 500 MHz at a variety of low altitudes and low flight speeds. The profile recorded along line WW-4C (Fig. 2) with the 200-MHz transducer is shown in Figure 5. All of the diffraction patterns are thought to correspond with crevasse features, the reverberation being caused by multiple reflections and several sharp transitions within the crevasses. Most notable is the strong hyperbola in the center of the record that seems to originate deep within the crevasse due to its 90-ns delay from the surface. In addition, dipping snow stratigraphy can be seen above the prominent hyperbolas. The separation between points where the dip begins allows crevasse width to be estimated (about 15 m for the large event at the center of the record). On the left side of the profile can be seen the gently sloping reflection from the snow surface as the aircraft altitude decreases. Data recorded during the approach show distinctive subsurface layering, fewer crevasse responses at depth, and little distortion of the near-surface layers associated with snow-bridges.

Three additional long lines, 4 to 5 km in length (Fig. 2), were profiled at an altitude of 10 m and a speed of 15 m s^{-1} to help define the areal extent of crevasses in this location. All of these profiles (not shown) reveal sloping and distorted layering interrupted by diffractions from crevasses. Profile WI-19 crosses the site from west to east and the purported tractor location was marked on the profile. Strong diffractions are found at the tractor location, but they do not seem unusual in comparison with the responses from other crevasses.

White Island speed study

The objective of this study was to determine if the radar could maintain its ability to record crevasse diffractions as the speed of the aircraft increased. A 2.2-km line (WI-15, Fig. 2) was established northeast of White Island in an area of large, widely spaced crevasses. Some of the crevasses, made apparent by snow bridge failure, were up to 8 m across and estimated to be 30 m deep. GPS coordinates were recorded at the line ends and midpoint. These stations were also flagged to help position the aircraft in this featureless terrain. Radar data were then collected at 51.2 scans/second from west to east using the 200-MHz transducer at an altitude of about 7 m and speeds of approximately 5, 10, and 20 m s^{-1}. In terms of distance the data rates are 10, 5, and 2.5 scans/m, respectively.

A segment of the profile recorded at 20 m s^{-1} is shown in Figure 6. Diffractions originating from large crevasses are clearly visible while responses from smaller crevasses and cracks are not adequately displayed on the reproduction.

Black Island traverse

The objective of this study was to establish the

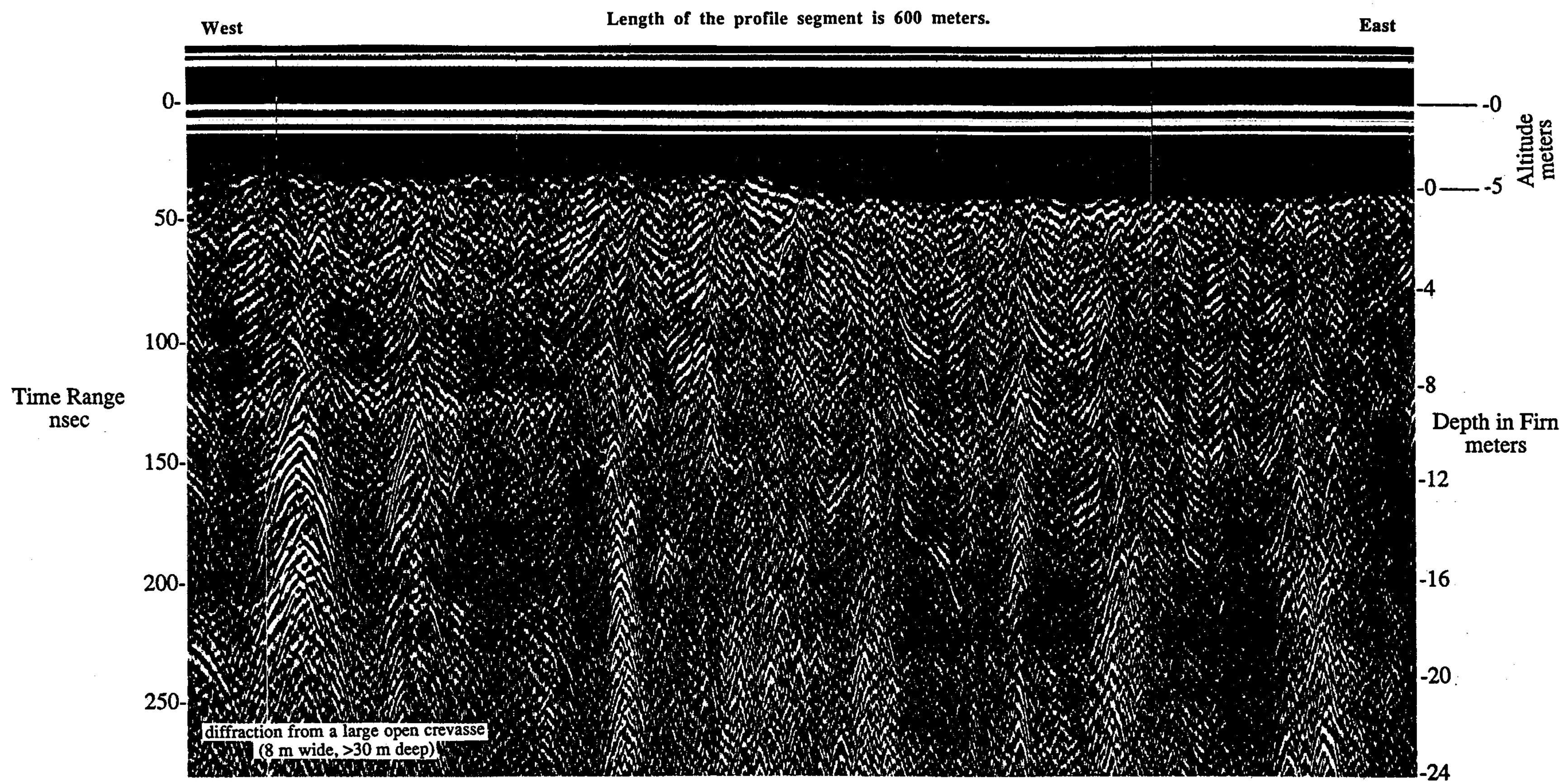

Figure 6. Segments of profiles recorded at different speeds above large crevasses on line WI-15 north of White Island. Diffractions seen at 5 m s^{-1} are still prominent at 20 m s^{-1}.

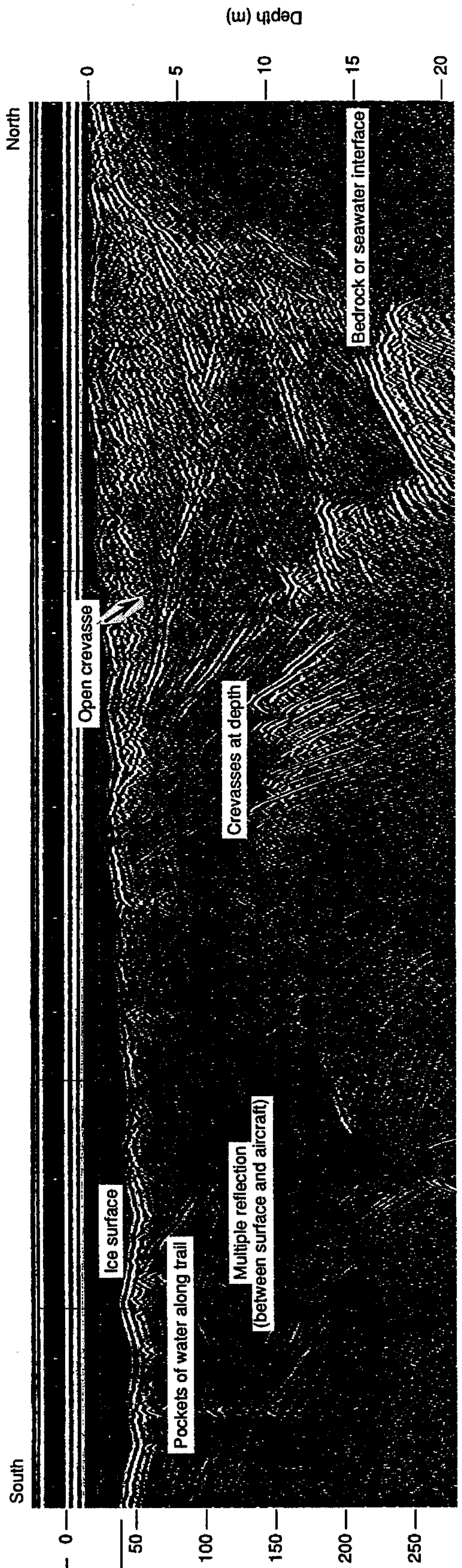

Figure 7. Profile recorded along the tractor traverse between White and Black Islands. This is an area of hard ice where crevassing was not expected.

nature of ice shelf profiles for a section apparently free of crevasses. A 200-MHz, 800-m profile (BI-1, Fig. 2) was recorded along the tractor trail between Black and White Islands with a single known crevasse that is crossed by a wooden bridge. This is an area of hard ice and high wind, and the ice surface along the tractor trail had little snow accumulation. Ice flow is from south to north between the islands. GPS waypoints were recorded incrementally along with the radar data. Survey altitude was about 5 m and airspeed 8 m s^{-1}.

The radar profile is shown in Figure 7. The small, near-surface diffractions at the start of the profile may originate from meltwater pools reported to exist along the tractor trail. Several distinct reflections are seen near the center of the record at a time depth of 100 ns (8.4 m). A possible explanation may be that shelf ice, moving northward, is overriding a sub-ice bedrock rib extending between the two islands, causing the ice to crack. This series of significant diffractions, in the area of the only known crevasse, may represent subsurface voids that have not yet been manifested at the ice surface. The diffraction from the open crevasse, indicated by the arrow on Figure 7, is overshadowed by reflections that could originate from a bedrock surface or seawater interface on top of the rock. The amplitude of the pulses reflected from this near-horizontal reflector is much higher than any other pulse amplitude originating from within the ice. The phase polarity of these reflections (Arcone 1994) indicates a material with dielectric permittivity higher than that of ice. The first 170 ns of the first 300 m of the record is free of the characteristic diffraction patterns associated with crevasses, and of reflections associated with layering seen at other sites.

Aurora Glacier and White Island transitions

The objective of this portion of the study was to look for transitions from crevassed to uncrevassed ice along probable flow lines in the ice shelf. Such transitions could indicate if transverse crevasses gradually close as the ice flows onto the shelf. Profiles were recorded along assumed flow lines. These lines coincided with the strike of undulations seen on the ice shelf that may indicate compression transverse to the flow direction. One 13-km-long profile (WB-1) extended from the terminus of the Aurora Glacier north onto the Ross Ice Shelf, and two profiles (10 and 12 km in length, WI-16 and WI-20, respectively) extended from glacial ice on the eastern end of White Island onto the Ross

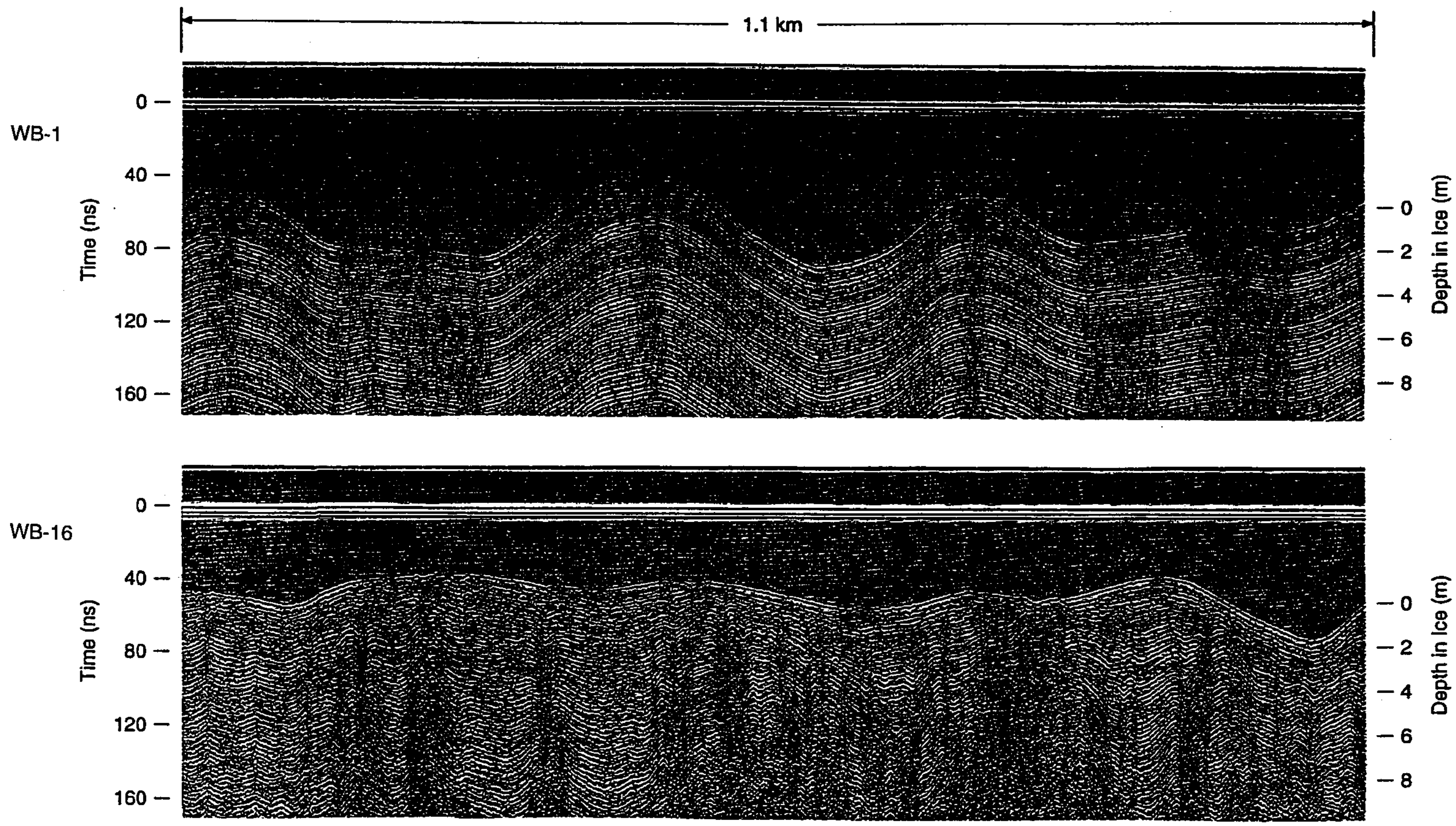

Figure 8. Segments of 500-MHz data files recorded near the terminus of the Aurora Glacier (top) and east of White Island (bottom). The event marks correspond with GPS waypoints spaced every 30 seconds. The undulations in position of the surface return represent changes in aircraft altitude.

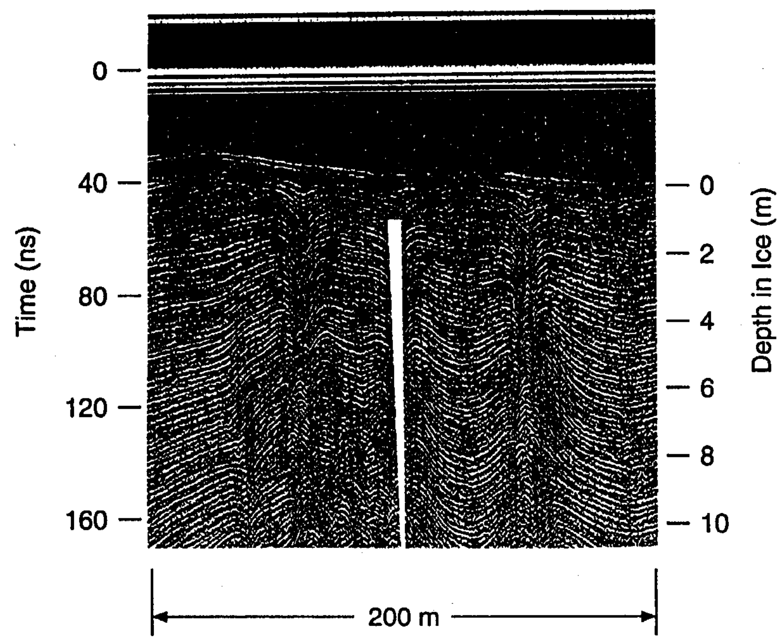

Figure 9. Unstacked segment of data recorded on White Island Profile (WI-18) showing in detail the density layer reflections and crevasse diffractions.

Ice Shelf (Fig. 2). Poor visibility near the terminus of the Aurora Glacier obscured the surface, and data were recorded at 10 to 15 m s^{-1} and 8-m altitude by following a compass heading. Profiles were collected for 10 minutes of flight using the 500-MHz transducer at 51.2 scans/second and a time range of 200 ns. GPS waypoints were recorded every 30 seconds. We then moved to the White Island area where light conditions were more favorable for low level work.

The lengths of the records preclude their complete presentation and data compression results in loss of resolution. Therefore, two typical data segments (one and one-half minutes in length) are shown (Fig. 8). The top segment was recorded near the terminus of the Aurora Glacier. The long period oscillation is due to the changes in aircraft altitude. The entire record is characterized by reflections from layering in the snow and ice, and no diffractions indicative of vertical interfaces are seen.

In contrast, the profile recorded east of White Island (bottom of Fig. 8) shows the continuity of the reflections from layering in the snow and ice to be interrupted by diffraction patterns and distorted stratigraphy associated with crevasses. Figure 8a should also be compared with data recorded along the Black Island traverse where no layering is seen.

An unstacked data segment from profile WI-18 (Fig. 9) shows the reflections associated with the crevasses more clearly. Layers within the ice are deformed near the crevasses, appearing to bend downward toward the voids. A crevasse drawn to scale is superimposed on the record.

CONCLUSIONS

Airborne short-pulse radar surveys are capable of detecting snow-bridged crevasses in cold snow and ice and could be used in a reconnaissance mode to map transitions in ice conditions. Crevasse responses are characterized by both diffractions and distortions in the snow-bridge stratigraphy. Observations along the control line show that diffractions can originate at any depth within crevasses where sharp transitions in dielectric permittivity occur. A large crevasse not visible from surface expression was detected with the radar and later excavated to measure snow-bridge thickness and the shape of the void.

Large crevasses were easily detected at speeds up to 20 m s^{-1} (45 mph), while information on the structure within individual snow bridges was revealed using the 500-MHz transducer at 5 m s^{-1} (11 mph). The 200-MHz transducer was superior for detecting crevasses but did not provide the best

information on snow-bridge thickness as the diffractions seemed to originate from deep within the crevasse.

Altitude should be restricted to 30 m or less because of time range-sampling restrictions and antenna beam spreading. Highly directive antennas should not be used because they would not pick up the tails of the diffractions. Altitude changes, during the survey, are actually desirable as they allow aircraft reflections to be easily filtered while still retaining the ice data.

A recently developed digital short-pulse radar system could be used for fairly rapid 64-m s^{-1} (140-mph) reconnaissance surveys on the Ross Ice Shelf to distinguish areas of ice that contain crevasses. To achieve the high scan rate (160 scans/sec), data are written directly to disk and would require post-flight processing. This information, along with GPS positioning, could be used for preliminary route corridor planning. The reconnaissance survey should be followed by a detailed airborne radar survey of the previously defined corridor to aid in final traverse positioning. For additional safety, the lead traverse vehicle should utilize a surface-mounted radar until the route is well established.

LITERATURE CITED

Arcone, S.A. (1994) Short-pulse radar wavelet recovery and resolution of dielectric contrast within englacial and basal ice of Matanuska Glacier, Alaska. (in prep)

Arcone, S.A., and A.J. Delaney (1987) Airborne river-ice thickness profiling with helicopter-borne UHF short pulse radar. *Journal of Glaciology,* **33**(115): 330–340.

Arcone, S.A. (1991) Dielectric constant and layer-thickness interpretation of helicopter-borne short-pulse radar waveforms reflected from wet and dry river-ice sheets. *IEEE Transactions on Geoscience and Remote Sensing,* **29**(5): 768–777.

Arcone, S.A., A.J. Delaney, and R.H. Wills (1992) Helicopter-borne alpine glacier surveys using short pulse radar. Geological Survey of Canada Paper 904, p. 25–32.

Arcone, S.A., A.J. Delaney, and D.J. Calkins (1989) Water detection in the coastal plains of the Arctic National Wildlife Refuge using helicopter-borne short pulse radar. U. S. Army Cold Regions Research and Engineering Laboratory, Hanover, New Hampshire. CRREL Report 89-7.

Cumming, W.A. (1952) The dielectric properties of ice and snow at 3.2 cm. *Journal of Applied Physics,* **23** (7): 768–773.

Delaney, A.J., S.A. Arcone, and E.F. Chacho (1990) Winter short-pulse radar studies on the Tanana River, Alaska. *Arctic,* **43**(3): 244–250.

Kovacs, A. (1977) Sea ice thickness profiling and under-ice oil entrapment. In *Proceedings, Offshore Technology Conference, Houston, Texas,* Paper 2949.

Kovacs, A. (1978) Remote detection of water under ice-covered lakes on the North Slope of Alaska. *Arctic,* **31**(4): 448–458.

Kovacs, A., and G. Abele (1974) Crevasse detection using an impulse radar system. *Antarctic Journal of the United States,* **9**(4): 177–178.

Kovacs, A., A.J. Gow, J.H. Cragin, and R.M. Morey (1982) The brine zone in the McMurdo Ice Shelf, Antarctica. U.S. Army Cold Regions Research and Engineering Laboratory, Hanover, New Hampshire. CRREL Report 82-39.

Kovacs, A., A.J. Gow, and R.M. Morey (1993) A reassessment of the in-situ dielectric constant of polar firn. U.S. Army Cold Regions Research and Engineering Laboratory, Hanover, New Hampshire. CRREL Report 93-26.

Vickers, R.S., J.E. Heighwa, and R.T. Gedway (1973) Airborne profiling of ice thickness using short-pulse radar. NASA Technical Memorandum (NASA-TM-X-71481).

Appendix A: Global Positioning System GPS Stations.

During these airborne studies, a coarse-acquisition GPS receiver (Garmin 100) was used for survey position control. An external GPS antenna was mounted on top of the radar transducer. The Garmin position coordinates were periodically compared with position coordinates displayed on the aircraft GPS and found to be in close agreement. The recorded position waypoints coincide with event markers on the radar profiles. Waypoints were recorded at the beginning and ends of lines at the Ice Fall, White Island tractor, and White Island speed sites. On all remaining long profiles, waypoints were recorded at 30-second intervals. Listed below are all of the radar lines and corresponding GPS waypoints.

Ice Fall Site

IF1	S 77° 49.50′	E 166° 45.55′
IF10	S 77° 49.48′	E 166° 46.05′
IF11	S 77° 49.45′	E 166° 46.07′
IE12	S 77° 49.41′	E 166° 46.02′
IF13	S 77° 49.37′	E 166° 46.03′
IE14	S 77° 49.33′	E 166° 46.04′
IF15	S 77° 49.30′	E 166° 46.04′
IF16	S 77° 49.27′	E 166° 46.07′
IF2	S 77° 49.47′	E 166° 45.47′
IF3	S 77° 49.43′	E 166° 45.53′
IF4	S 77° 49.40′	E 166° 45.58′
IF5	S 77° 49.38′	E 166° 45.57′
IF6	S 77° 49.34′	E 166° 45.55′
IF7	S 77° 49.31′	E 166° 45.65′
IF8	S 77° 49.26′	E 166° 45.75′
IF9	S 77° 49.51′	E 166° 46.04′
PEG01	S 77° 54.81′	E 166° 45.35′
PEB02	S 77° 54.51′	E 166° 47.73′
PEG03	S 77° 54.15′	E 166° 50.52′

White Island Tractor Site

WI10	S 77° 57 20′	E 168° 32 75′
WI10A	S 77° 57.22′	E 168° 32.78′
WI11	S 77° 56.93′	E 168° 32.76′
WI11A	S 77° 56.93′	E 168° 32.81′
WI12	S 77° 56.95′	E 168° 32.86′
WI13	S 77° 56.96′	E 168° 32.93′
WI14	S 77° 56.97′	E 168° 32.98′
WI15	S 77° 56.97′	E 168° 33.03′
WI16	S 77° 56.98′	E 168° 33.07′
WI17	S 77° 56.99′	E 168° 33.12′
WI18	S 77° 56.99′	E 168° 33.17′
WI19	S 77° 57.01′	E 168° 33.24′
WI1A	S 77° 57.09′	E 168° 32.32′
WI2	S 77° 57.08′	E 168° 32.40′
WI20	S 77° 57.02′	E 168° 33.32′
WI20A	S 77° 57.03′	E 168° 33.25′
WI3	S 77° 57.11′	E 168° 32.46′
WI4	S 77° 57.12′	E 168° 32.51′
WI5	S 77° 57.15′	E 168° 32.57′
WI6	S 77° 57.16′	E 168° 32.62′
WI7	S 77° 57.18′	E 168° 32.68′
WI8	S 77° 57.19′	E 168° 32.72′
WI9	S 77° 57.20′	E 168° 32 75′

White Island Speed Survey Site

WW1	S 78° 12.83′	E 167° 33.52′
WW2	S 78° 12.49′	E 167° 35.50′
WW3	S 78° 12.11′	E 167° 37.82′
WW3A	S 78° 12.11′	E 167° 37.85′
277	S 78° 13.85′	E 166° 47.01′
278	S 77° 38.03′	E 167° 38.02′
279	S 77° 38.46′	E 167° 38.80′
280	S 77° 38.81′	E 167° 39.36′
281	S 77° 39.12′	E 167° 39.71′
282	S 77° 39.46′	E 167° 40.12′
283	S 77° 39.79′	E 167° 40.60′
284	S 77° 40.17′	E 167° 40.97′
285	S 77° 40.52′	E 167° 41.40′
286	S 77° 41.18′	E 167° 41.94′
287	S 77° 41.49′	E 167° 42.51′
288	S 77° 41.72′	E 167° 42.91′
289	S 77° 41.95′	E 167° 43.20′
290	S 77° 42.15′	E 167° 43.37′
291	S 77° 42.37′	E 167° 43.63′
292	S 77° 42.68′	E 167° 44.04′
293	S 77° 42.98′	E 167° 44.48′
294	S 77° 43.33′	E 167° 44.86′
295	S 77° 43.66′	E 167° 45.38′
296	S 77° 43.99′	E 167° 45.98′
297	S 77° 44.30′	E 167° 46.56′
298	S 77° 44.62′	E 167° 47.15′

White Island (WI20)

299	S 78° 03.75′	E 167° 57 02′
300	S 78° 03.90′	E 167° 56.12′
301	S 78° 04.12′	E 167° 54.98′
302	S 78° 04.34′	E 167° 53.94′
303	S 78° 04.55′	E 167° 52.96′
304	S 78° 04.77′	E 167° 52.06′
305	S 78° 04.99′	E 167° 51.20′
306	S 78° 05.21′	E 167° 50.34′
307	S 78° 05.42′	E 167° 49.46′
308	S 78° 05.65′	E 167° 48.59′
309	S 78° 05.89′	E 167° 47.80′
310	S 78° 06.14′	E 167° 46.95′
311	S 78° 06.39′	E 167° 46.16′
312	S 78° 06.64′	E 167° 45.40′
313	S 78° 06.88′	E 167° 44.63′
314	S 78° 07.14′	E 167° 43.81′
315	S 78° 07.39′	E 167° 42.98′
316	S 78° 07.65′	E 167° 42.00′
317	S 78° 07.90′	E 167° 40.91′

White Island (WI16)

318	S 78° 08 14′	E 167° 39 83′
319	S 78° 08.62′	E 167° 34.81′
320	S 78° 08.39′	E 167° 36.26′
321	S 78° 08.17′	E 167° 37.34′
322	S 78° 07.96′	E 167° 38.57′
323	S 78° 07.74′	E 167° 39.63′
324	S 78° 07.15′	E 167° 43.11′
325	S 78° 06.97′	E 167° 44.20′
326	S 78° 06.77′	E 167° 45.28′
327	S 78° 06.57′	E 167° 46.25′
328	S 78° 06.37′	E 167° 47.42′
329	S 78° 06.18′	E 167° 48.58′
330	S 78° 05.97′	E 167° 49.80′
331	S 78° 05.77′	E 167° 50.90′
332	S 78° 05.57′	E 167° 52.13′
333	S 78° 05.37′	E 167° 53.29′

White Island (WI17)

334	S 77° 55.87′	E 168° 32.20′
335	S 77° 56.21′	E 168° 32.20′
336	S 77° 56.49′	E 168° 32.31′
337	S 77° 57.27′	E 168° 32.58′
338	S 77° 57.52′	E 168° 32.85′
339	S 77° 57.79′	E 168° 33.11′
340	S 77° 58.05′	E 168° 33.35′

White Island (WI18)

341	S 77° 58.05′	E 168° 33.48′
342	S 77° 57.74′	E 168° 32.80′
343	S 77° 57.32′	E 168° 31.96′
344	S 77° 56.92′	E 168° 32.14′
345	S 77° 56.56′	E 168° 32.84′
346	S 77° 56.31′	E 168° 33.86′
347	S 77° 56.03′	E 168° 34.55′

White Island (WI19)

348	S 77° 56.71′	E 168° 37.04′
349	S 77° 56.80′	E 168° 35.50′
350	S 77° 56.90′	E 168° 34.09′
351	S 77° 57.03′	E 168° 32.72′
352	S 77° 57.13′	E 168° 31.55′
353	S 77° 57.22′	E 168° 30.18′
354	S 77° 57.32′	E 168° 28.82′
355	S 77° 57.42′	E 168° 27.36′
356	S 77° 57.55′	E 168° 25.69′

Black Island Traverse

BI1	S 78° 13 27′	E 166° 47 66′
BI10	S 78° 13.61′	E 166° 46.64′
BI11	S 78° 13.65′	E 166° 46.58′
BI12	S 78° 13.67′	E 166° 46.53′
BI13	S 78° 13.70′	E 166° 46.47′
BI14	S 78° 13.73′	E 166° 46.43′
BI2	S 78° 13.33′	E 166° 47.38′
BI3	S 78° 13.37′	E 166° 47.13′
BI4	S 78° 13.42′	E 166° 46.96′
BI5	S 78° 13.45′	E 166° 46.91′
BI6	S 78° 13.47′	E 166° 46.87′
BI7	S 78° 13.50′	E 166° 46.83′
BI8	S 78° 13.53′	E 166° 46.77′
BI9	S 78° 13.58′	E 166° 46.69′

REPORT DOCUMENTATION PAGE

Form Approved
OMB No. 0704-0188

1. AGENCY USE ONLY (Leave blank)

2. REPORT DATE
March 1995

3. REPORT TYPE AND DATES COVERED

4. TITLE AND SUBTITLE
Detection of Crevasses Near McMurdo Station, Antarctica With Airborne Short-Pulse Radar

5. FUNDING NUMBERS
National Science Foundation
Grant No. DPP-872 0064

6. AUTHORS

Allan J. Delaney and Steven A. Arcone

7. PERFORMING ORGANIZATION NAME(S) AND ADDRESS(ES)
U.S. Army Cold Regions Research and Engineering Laboratory
72 Lyme Road
Hanover, N.H. 03755-1290

8. PERFORMING ORGANIZATION REPORT NUMBER
Special Report 95-7

9. SPONSORING/MONITORING AGENCY NAME(S) AND ADDRESS(ES)
Division of Polar Programs
National Science Foundation
Arlington, Virginia 22230

10. SPONSORING/MONITORING AGENCY REPORT NUMBER
PR: T-310

11. SUPPLEMENTARY NOTES

12a. DISTRIBUTION/AVAILABILITY STATEMENT
Approved for public release; distribution is unlimited.
Available from NTIS, Springfield, Virginia 22161

12b. DISTRIBUTION CODE

13. ABSTRACT (*Maximum 200 words*)

Airborne short-pulse radar is evaluated experimentally as a rapid reconnaissance tool for locating snow-bridged crevasses. An immediate need for a crevasse detector is present within the U.S. Antarctic Program, which is planning a major surface traverse from McMurdo to deliver construction materials to South Pole Station. This feasibility study of a crevasse detection system was performed near McMurdo Station, Antarctica, in January 1994. The radar utilized pulses centered near 200 and 500 MHz and was operated from a low flying helicopter with altitude and speed as variables. A global positioning system (GPS) was used for survey control. Results are presented over glacial ice on Ross Island and at various locations on the Ross Ice Shelf near White and Black Islands and near the Aurora Glacier terminus. These studies include a control line along which crevasse width and snow-bridge thickness were measured, transects along which crevasses were apparent, and also where crevasses were expected, but were not apparent. Strong evidence of crevassing was recorded at flight speeds near 20 m s^{-1} (45 mph), at altitudes near 15 m, and at a data acquisition rate of 51 scans/second. Crevasses are detected by the reflections and diffractions from distorted layering in snow bridges, and by the strong diffractions from within the crevasses. The strongest diffractions apparently emanated from within the crevasse and not from the base of the snow bridge. Along the control line, a crevasse with no surface expression was detected by radar and verified by probing and digging. Transects devoid of crevasses show layering without the small scale distortion seen over snow bridges. Future plans are to use data acquisition rates of 160 scans/second, available with commercial equipment, to allow a survey speed of about 64 m s^{-1} (140 mph). We believe that quality data could then be acquired at altitudes up to about 30 m, making short pulse radar a useful crevasse mapping tool from fixed wing aircraft.

14. SUBJECT TERMS

Antarctica	McMurdo Station	Snow
Crevasse detection	Ross Ice Shelf	
Ice	Short-pulse radar	

15. NUMBER OF PAGES
20

16. PRICE CODE

17. SECURITY CLASSIFICATION OF REPORT	18. SECURITY CLASSIFICATION OF THIS PAGE	19. SECURITY CLASSIFICATION OF ABSTRACT	20. LIMITATION OF ABSTRACT
UNCLASSIFIED	UNCLASSIFIED	UNCLASSIFIED	UL